Antibubble dynamics: slipping or viscous interfaces?

P1. Benoit Scheid[a], P2. Stéphane Dorbolo[b]

a. *TIPs - Fluid Physics unit, Université Libre de Bruxelles C.P. 165/67, 1050 Brussels, Belgium, EU*
b. *GRASP, Physics Department B5, Université de Liège, 4000 Liège, Belgium, EU*

Abstract :

An antibubble is a spherical thin air shell that is immersed in a water-surfactant mixture and drains under the action of hydrostatic pressure. A lubrication model has been built and account for either slipping or shear viscosity at the shell interfaces. Numerical solutions show a plug (resp. Poiseuille) flow for large (resp. small) slip length or alternatively for small (resp. large) surface shear viscosity. Comparison of antibubble lifetimes with available experimental data is clearly in favor of the surface viscosity model.

Résumé :

Une antibulle est une 'coquille' sphérique faite d'un film d'air mince, immergée dans une solution eau-surfactants, et étant le siège d'un écoulement sous l'action de la pression hydrostatique. Un modèle de lubrification est proposé pour rendre compte soit d'un glissement, soit d'une viscosité de cisaillement aux interfaces de cette 'coquille'. Les solutions numériques montrent un écoulement type bouchon (resp. Poiseuille) pour une grande (resp. petite) longueur de glissement ou alternativement pour une petite (resp. grande) viscosité de cisaillement de surface. La comparaison des temps de vie des antibulles avec des données expérimentales joue clairement en faveur du modèle de viscosité de surface.

Mots clefs : **Thin film flows ; Foams ; Surface viscosity**

1 Introduction

Foams are often used under various flow regimes, whose specific applications in technological processes rely essentially on their properties. Among these, the rheological properties are probably today the most challenging ones to be modeled (see *e.g.* Emile et al. (2009)). In foam dynamics as in most of dynamical systems involving fluid-fluid interfaces with surface-active materials, both surface viscosity and elasticity, with both shear and dilatational components, are often indissociable, which makes the physical interpretation difficult, if not impossible. Still for some specific flow regime and appropriate surfactant solution, conditions can be reached where only one effect is isolated from the others. Scheid et al. (2010) have recently shown in the Landau-Levich-Derjaguin coating problem that the thickness of deposited films obtained with very soluble surfactant and at concentration far above the critical micellar concentration could be rationalized by the sole effect of surface shear viscosity. We believe that similar conditions can be obtained in other configurations and that antibubbles are among them.

An antibubble is a spherical air shell surrounded by liquid (see *e.g.* Dorbolo et al. (2005) and references therein). It is an ephemeral object as the air drains driven by the hydrostatic pressure difference along the air shell. Recently, Dorbolo et al. (2010) have shown that the surface modulus of the mixture has a strong influence on the lifetime of an antibubble. These experimental results were obtained at concentration much above the cmc for which the interfaces are strongly immobilized by the presence of surfactants (see *e.g.* Stebe et al. (1991)). Hence the first estimate of antibubble lifetimes has been obtained from a lubrication model of the air film assuming the liquid surfaces to be perfectly immobile, i.e. considering no-slip boundary conditions at the 'liquid wall' (Dorbolo et al. (2005)). However, the corresponding lifetimes are of the order of an hour, while measured lifetimes are instead of the order

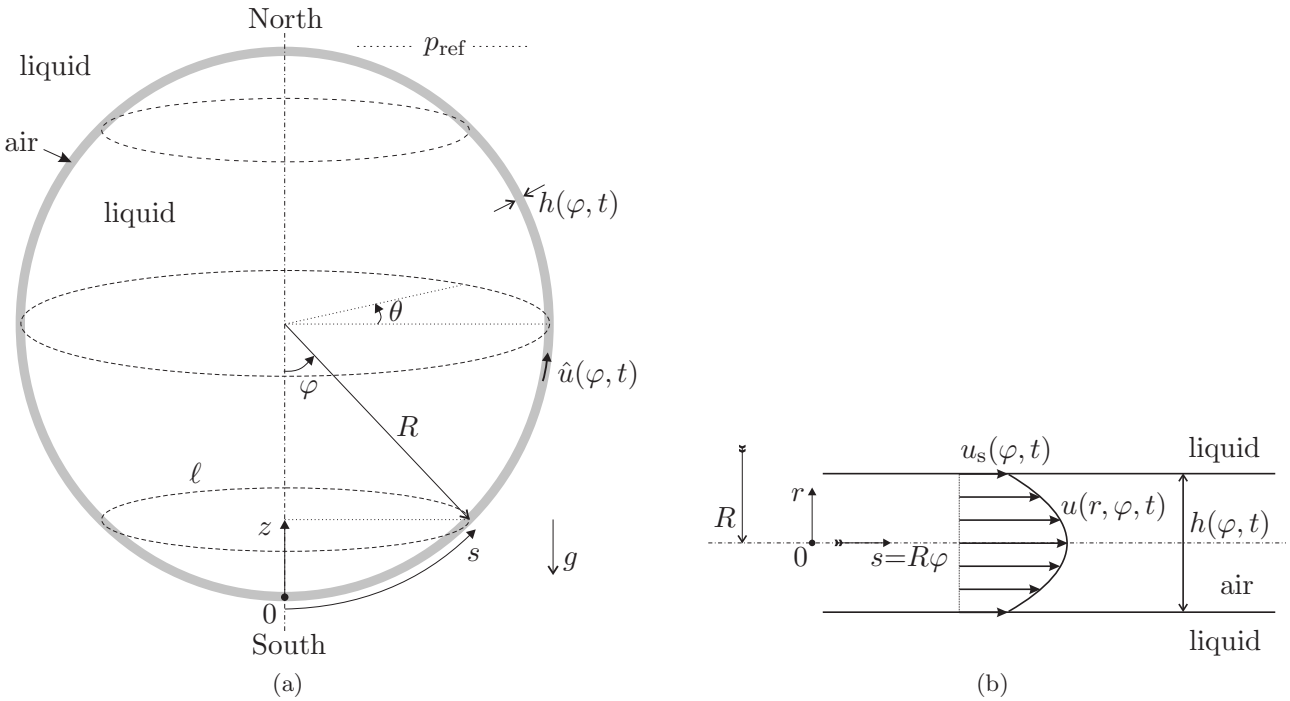

FIG. 1 – (a) Sketch of an antibubble. (b) Zoom of the film flow of air.

of a minute provided the surfactant mixture has a high surface modulus (Dorbolo et al. (2010)). For the air film to drain faster than if it was between two solid plates, the surface velocity should be larger than zero and in the same direction than the drainage. In the present paper, we therefore consider two physical mechanisms that allow for non-zero surface velocities, namely slip and surface viscosity, and try to discriminate between them in regard to available experimental data.

2 Problem formulation

We model an antibubble as a spherical air film of constant radius R surrounded by a liquid, as sketched in Fig. 1(a). As in a soap bubble, the sphericity of the antibubble is ensured by the excess of capillary pressure in the liquid trapped by the film relative to the liquid outside. The Laplace pressure drop across each interface is $2\gamma/R$, where γ is the air-liquid interfacial tension. We assume the problem to be symmetric around the z-axis, i.e. uniform in the azimuthal direction θ. The thickness of the film is denoted by h and depends on time t and on the polar coordinate $\varphi \in [0,\pi]$, or alternatively the curvilinear coordinate $s = R\varphi$, that has its origin at the South pole. The air in the film is assumed to be incompressible and flows against gravity due to the hydrostatic pressure difference between the poles, namely $p_0 = 2\rho g R$, where ρ is the liquid density and g the gravitational acceleration. Nevertheless, the pressure gradient is nonlinear in φ, being maximum at the equator and vanishing at the poles. Therefore, at any vertical position $z = R\,(1-\cos\varphi)$ above the South pole (see Fig. 1), the hydrostatic pressure difference, relative to the reference pressure $p_{\rm ref}$, has the form

$$p_{\rm hyd} = \rho g(2R - z) = \rho g R\,(1+\cos\varphi)\ . \tag{1}$$

Denoting $\hat{u}(\varphi,t)$ the average air velocity in the film, the mass conservation equation $\partial_t h + \nabla\cdot(h\hat{u}) = 0$ becomes in spherical coordinates :

$$\frac{\partial h}{\partial t} + \frac{1}{R\sin\varphi}\frac{\partial}{\partial\varphi}\left(\sin\varphi\, h\hat{u}\right) = 0\ . \tag{2}$$

The average velocity $\hat{u}$ is determined by solving the Navier-Stokes (NS) equation in the air film assuming azimuthal symmetry. Moreover, the thickness h of the film being much smaller than the

characteristic length $L = \pi R$ in the flow direction, the problem reduces to the resolution of the lubrication equation, which is written here at leading order in the asymptotic expansion of the NS equations based on the parameter $\varepsilon = r/R \ll 1$:

$$\mu_{\rm air}\frac{\partial^2 u}{\partial r^2} = \frac{1}{R}\frac{\partial p}{\partial \varphi}\,, \tag{3}$$

where $\mu_{\rm air}$ is the dynamic viscosity, r the transverse coordinate with the origin at the centerline of the film as represented in Fig. 1(b), $u(r,\varphi,t)$ the velocity field and $p(\varphi,t)$ the pressure field. Solving (3) with the symmetry condition $\partial_r u = 0$ at $r = 0$ and the surface velocity $u = u_{\rm s}(\varphi,t)$ at $r = h/2$, yields

$$u(r,\varphi,t) \;=\; u_{\rm s} - \frac{1}{2\mu_{\rm air}R}\frac{\partial p}{\partial \varphi}\left(\frac{h^2}{4} - r^2\right) \tag{4}$$

$$\hat{u}(\varphi,t) \;\equiv\; \frac{2}{h}\int_0^{h/2} u\,{\rm d}r = u_{\rm s} - \frac{h^2}{12\mu_{\rm air}R}\frac{\partial p}{\partial \varphi}\,. \tag{5}$$

The capillary pressure in the air film, $p_{\rm cap}$, does not only depend on the mean curvature $(1/R)$ of the antibubble but also on local variation of the film curvature, denoted $K(h)$, which reduces to $K = \Delta(h/2)/2$ in the frame of the lubrication approximation ($\nabla h \ll 1$). Therefore, the total pressure and its gradient in the film, using (1), become

$$p \;\equiv\; p_{\rm ref} + p_{\rm hyd} + p_{\rm cap} = p_{\rm ref} + \rho g R(1+\cos\varphi) + 2\gamma\left(\frac{1}{R} - K(h)\right)\,, \tag{6}$$

$$\frac{\partial p}{\partial \varphi} \;=\; -\rho g R\sin\varphi - \frac{\gamma}{2}\frac{\partial}{\partial\varphi}(\Delta h) \qquad \text{where} \qquad \Delta h = \frac{1}{R^2\sin\varphi}\frac{\partial}{\partial\varphi}\left(\sin\varphi\frac{\partial h}{\partial\varphi}\right)\,. \tag{7}$$

Defining the characteristic timescale $\tau = \mu_{\rm air}\pi^2 R/(\rho g h_0^2)$ over which the lubrication flow takes place, where h_0 is the average initial thickness, the non-dimensionalization is performed through the scaling

$$h = h_0\bar{h}\,, \quad r = h_0\bar{r}\,, \quad t = \tau\bar{t}\,, \quad \varphi = \pi\bar{\varphi} \quad s = L\,\bar{s}\,, \quad u = \frac{L}{\tau}\bar{u} \quad \text{and} \quad p = p_0\bar{p}\,. \tag{8}$$

The conservation equation (2), combined with (5) and (7), becomes in dimensionless form :

$$\frac{\partial\bar{h}}{\partial\bar{t}} + \frac{1}{\sin(\pi\bar{\varphi})}\frac{\partial}{\partial\bar{\varphi}}\left[\bar{h}\sin(\pi\bar{\varphi})\left(\bar{u}_{\rm s} - \frac{\bar{h}^2}{6}\frac{\partial\bar{p}}{\partial\bar{\varphi}}\right)\right] = 0\,, \tag{9a}$$

$$\text{with} \qquad \frac{\partial\bar{p}}{\partial\bar{\varphi}} = -\frac{\pi}{2}\sin(\pi\bar{\varphi}) - Bo\frac{\partial}{\partial\bar{\varphi}}\left(\frac{1}{\sin(\pi\bar{\varphi})}\frac{\partial}{\partial\bar{\varphi}}\left[\sin(\pi\bar{\varphi})\frac{\partial\bar{h}}{\partial\bar{\varphi}}\right]\right)\,, \tag{9b}$$

where $Bo = \gamma h_0/(4\rho g\pi^2 R^3)$ is the Bond number that measures the importance of the capillary pressure relative to the hydrostatic pressure. Note that $\bar{\varphi} = \bar{s}$, that ranges between 0 and 1. Equations (9) should be solved with symmetric boundary conditions at the poles, namely

$$\frac{\partial\bar{h}}{\partial\bar{\varphi}} = 0 \qquad \text{and} \qquad \frac{\partial\bar{p}}{\partial\bar{\varphi}} = 0 \qquad \text{at} \qquad \bar{\varphi} = 0, 1\,. \tag{10}$$

Finally, the problem has to be closed by an equation for the surface velocity $\bar{u}_{\rm s}$. To this aim, two different stress boundary conditions at the interfaces accounting for the presence of surfactants are proposed hereafter, depending on whether the liquid surfaces are assumed to be slipping or viscous.

Slip boundary condition : Assuming a slip length λ at the interface, the stress boundary condition is $\lambda\,\mathbf{t}\cdot\boldsymbol{\sigma}\cdot\mathbf{n} = \mu_{\rm air}\,\mathbf{t}\cdot\mathbf{u}$, where $\mathbf{n}$ and $\mathbf{t}$ are, respectively, the outward normal and the tangential unit vectors, $\boldsymbol{\sigma}$ is the stress tensor and $\mathbf{u}$ the fluid velocity. In the frame of the lubrication approximation, i.e. for $r \ll R$, this condition at leading order reduces to

$$-\lambda\frac{\partial u}{\partial r}\Big|_{r=\frac{h}{2}} = u_{\rm s} \qquad \text{or} \qquad \bar{u}_{\rm s} = -\Lambda\bar{h}\frac{\partial\bar{p}}{\partial\bar{\varphi}}\,, \tag{11}$$

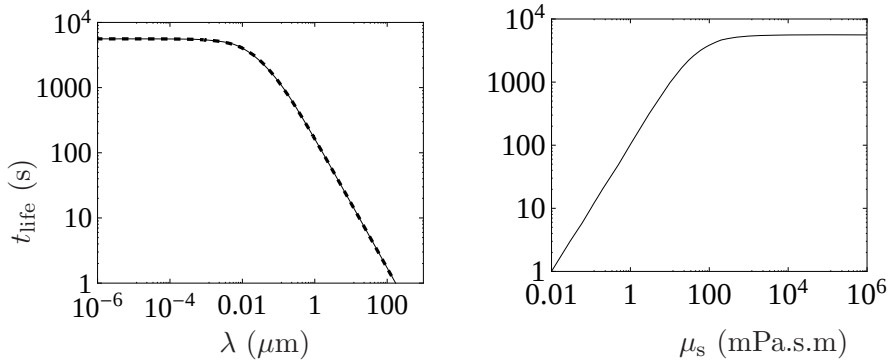

(a) Slip length (b) Surface shear viscosity

FIG. 2 – Antibubble lifetime obtained from simulations for $h_0 = 1\,\mu$m and $R = 1\,$cm : (a) computed with (12) (solid line) and with (15) (dotted line) ; (b) computed with (9-13).

where $\Lambda = \lambda/h_0$ is the dimensionless slip length. Replacing (11) in (9a) yields

$$\frac{\partial \bar{h}}{\partial \bar{t}} + \frac{1}{\sin(\pi\bar{\varphi})}\frac{\partial}{\partial \bar{\varphi}}\left[\sin(\pi\bar{\varphi})\left(-\frac{\bar{h}}{6} - \Lambda\right)\bar{h}^2\frac{\partial \bar{p}}{\partial \bar{\varphi}}\right] = 0\ . \tag{12}$$

Surface viscosity boundary condition : Assuming now a shear viscous stress at the liquid/gas interfaces (no dilatation or compression of the interfaces), inherent to the presence of surfactants, and defining $\mu_{\rm s}$ as the shear surface viscosity, the tangential stress boundary condition is $\mathbf{t}\cdot\boldsymbol{\sigma}\cdot\mathbf{n} = \mathbf{t}\cdot\boldsymbol{\nabla}_{\rm s}\left(\mu_{\rm s}\boldsymbol{\nabla}_{\rm s}\cdot\mathbf{u}\right)$ where $\boldsymbol{\nabla}_{\rm s} = (\mathbf{I}-\mathbf{nn})\cdot\boldsymbol{\nabla}$ is the surface gradient operator (see e.g. Naire et al. (2001)). In the frame of the lubrication approximation, i.e. for $r \ll R$, this condition at leading order reduces to

$$\mu_{\rm air}\frac{\partial u}{\partial r}\Big|_{r=\frac{h}{2}} = \frac{\mu_{\rm s}}{R^2}\frac{\partial}{\partial\varphi}\left(\frac{1}{\sin\varphi}\frac{\partial}{\partial\varphi}(\sin\varphi\, u_{\rm s})\right) \qquad \text{or} \qquad Bq\frac{\partial}{\partial\bar{\varphi}}\left(\frac{1}{\sin(\pi\bar{\varphi})}\frac{\partial}{\partial\bar{\varphi}}(\sin(\pi\bar{\varphi})\,\bar{u}_{\rm s})\right) = \bar{h}\frac{\partial\bar{p}}{\partial\bar{\varphi}}\ , \tag{13}$$

where $Bq = \mu_{\rm s}h_0/(\mu_{\rm air}\pi^2R^2)$ is the Boussinesq number that compares the shear surface viscosity with the shear bulk viscosity. Equation (13) should be solved with vanishing velocity at the poles, i.e.

$$\bar{u}_{\rm s} = 0 \qquad \text{at} \qquad \bar{\varphi} = 0, 1\ . \tag{14}$$

3 Time-dependent simulations

Numerical simulations have been performed using COMSOL® in order to explore the antibubble dynamics and determine the lifetime as function of the problem parameters. The antibubble is assumed to break up due to molecular interactions at the South pole, where the rupture film thickness is reached. Here we fix $h_{\rm rupt} = 100\,$nm. The computational domain is $\bar{\varphi} \in [0, 1]$ with a mesh size of 10^{-3}, refined to 10^{-4} at the poles. As initial condition, we assume a uniform film thickness, i.e. $\bar{h}(\bar{\varphi}, 0) = 1$. The liquid is a surfactant solution of density $\rho = 1000\,$kg/m^3 and surface tension $\gamma = 28.5\,$mN/m. The dynamic viscosity of air is $\mu_{\rm air} = 1.85\times10^{-5}\,$Pa.s. Results are outlined below for the slip and the surface viscosity models.

Slip model : Considering the slip condition at the air-liquid interfaces, we numerically solve the system (12,9b) together with the boundary conditions (10). Figure 2(a) shows the lifetime as a function of the slip length λ for an antibubble radius $R = 1\,$cm and an initial film thickness $h_0 = 1\,\mu$m. As the slip length increases the lifetime decreases drastically, covering a wide range of possible lifetimes.

As the film thins primarily at the South pole, we next rewrite (12) in the limit of $\bar{\varphi} \to 0$ with neglecting curvature gradient effects ($Bo = 0$). The result is an ordinary differential equation (ODE) for the space-independent thickness, i.e. $\bar{h} = \bar{h}_{\rm min}(t)$:

$$\frac{{\rm d}\bar{h}_{\rm min}}{{\rm d}\bar{t}} + \frac{\pi^2\bar{h}_{\rm min}^3}{6} = -\pi^2h_{\rm min}^2\Lambda\ . \tag{15}$$

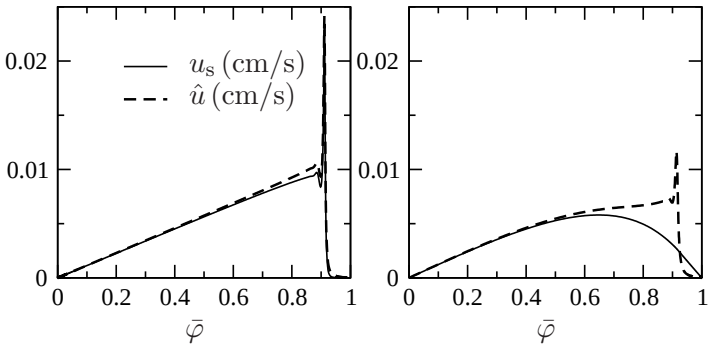

FIG. 3 – Surface and average velocities at rupture time ($t_{\rm life}$) obtained for both the slip (left) and the surface viscosity (right) models with $h_0 = 1\,\mu$m and $R = 1\,$cm. The values $\lambda = 1.36\,\mu$m (left) and $\mu_s = 1.17\,$mPa.s.m (right) have been chosen such that the lifetime is about 120 s in both cases.

For the no-slip limit ($\Lambda = 0$), the solution of (15) is given by

$$\bar{h}_{\rm rupt} \equiv \bar{h}_{\rm min}(\bar{t}) = \left(1 + \frac{\pi^2}{3}\,\bar{t}\right)^{-1/2} \qquad \text{or} \qquad t_{\rm life} = \frac{3\mu_{\rm air} R\left(1 - \frac{h_{\rm rupt}^2}{h_0^2}\right)}{\rho g h_{\rm rupt}^2}\,, \tag{16}$$

which reduces to $t_{\rm life}^{\infty} = 3\mu_{\rm air}R/(\rho g h_{\rm rupt}^2)$ for $h_{\rm rupt} \ll h_0$, as predicted by Dorbolo et al. (2005).

For $\Lambda \neq 0$, the ODE (15) should be solved numerically. The result is plotted in Fig. 2(a) (dashed line), which superimposes the numerical results obtained with the PDE (12). It demonstrates that the antibubble lifetime is entirely determined by the film dynamics in the vicinity of the South pole only.

Surface viscosity model : Considering the surface viscosity condition at the air-liquid interfaces, we numerically solve the system (9,13) together with the boundary conditions (10,14). Figure 2(b) shows the lifetime as a function of the surface viscosity μ_s for an antibubble radius $R = 1\,$cm and an initial film thickness $h_0 = 1\,\mu$m. The no-slip condition is recovered for $\mu_s \to \infty$. As the surface viscosity decreases, the lifetime decreases drastically, covering again a wide range of possible lifetimes.

4 Flow behavior

The simulation results obtained in the previous section with both the slip length and the surface viscosity models are qualitatively similar (see Fig. 2) and it remains to discriminate between these two models. In order to get insights into the intrinsic differences between the slip and the surface viscosity models, we plot in Fig. 3 the dimensional surface and average velocities obtained with each one. The values of the corresponding parameters have been chosen to obtain the same lifetime $t_{\rm life} \approx 120\,$s. For the slip model, the surface and average velocities are nearly identical, which indicates the presence of a "plug flow", i.e. a uniform velocity profile across the film. Furthermore, the velocity increases linearly up to the air pocket that forms at the North pole, in the vicinity of which it reaches a maximum. At the equator, the velocity is about $50\,\mu$m/s and has a maximum of about $200\,\mu$m/s near the North pole. For the surface viscosity model, the flow is also uniform in the South hemisphere while in the North hemisphere, the surface velocity monotonically decreases contrarily to the average velocity that has a peak, indicating the existence of a parabolic velocity profile in that region. Nevertheless, the qualitative difference of the flow behavior between the two models in the North hemisphere does not help to discriminate between the models as the lifetime only depends on the flow behavior in the vicinity of the South poles (see previous section).

5 Comparison to experimental data and concluding remarks

We now look at available experimental data by Dorbolo et al. (2010) who used the mixture SLES + CAPB + MAc proposed by Denkov and coworkers (see *e.g.* Golemanov et al. (2008)). The authors reported lifetimes ranging bewteen 100 and 300 s, which, following our models, corresponds either to

slip lengths ranging between 0.5 and 1.5 μm, or to surface shear viscosities ranging between 1 and 3 mPa.s.m, as deduced from Fig. 2.

Apparent slip lengths reported experimentally span many orders of magnitude, from molecular lengths up to hundreds of nanometers Lauga et al. (2007). It is found in Maali and Bhushan (2008) that the effective slip length for an air flow confined between two solid surfaces separated by a micrometer gap is about 100 nm at ambient pressure and temperature. To match the experimental data in Dorbolo et al. (2010), the slip length should only be one order of magnitude larger, which is possible provided the difference is ascribed to the presence of surfactants adsorbed at the liquid surfaces. Even though no direct measurements of slip of an air flow along surfactant-mixture surfaces are available, Kunert and Harting (2008) have shown that the slip length for a liquid flow over a solid substrate decreases with the concentration of surfactants adsorbed on the substrate. This is therefore consistent with the experimental observations in Dorbolo et al. (2010) that the antibubble lifetime increases with increasing surfactant concentration, hence decreasing slip length, as predicted by the slip model.

As for the slip length, no experimental measurements of the surface shear viscosity of the mixture SLES+CAPB+MAc has been performed, which also prevent to conclude about the surface viscosity model. Nevertheless, it has been reported that the antibubble lifetime increases with the surface modulus Dorbolo et al. (2010). Assuming there is a correlation between the surface modulus and the surface shear viscosity Stenvot and Langevin (1988), one gets from the surface viscous model that the antibubble lifetime approximately doubles as the surface viscosity doubles (at least in the linear region of Fig. 2b), exactly like in experiments. Additionally, Dorbolo et al. (2010) mentioned the great difficulty to generate an antibubble with a solution of SDS (as often used in soap films). Interestingly, surface shear viscosity for SDS solutions has been measured by Petkov et al. (1996) and is of the order of 10^{-3} mPa.s.m, which, following the surface viscosity model, gives lifetimes of the order of 1/100 s. This is at least consistent with experimental observations that no antibubble can be generated with SDS only. Now, the above arguments are only qualitative and cannot be used as proofs. Only measurements of shear surface viscosity of the mixture used in experiments will allow to conclude about the pertinence of the surface viscous model.

We thank the FRS-FNRS for funding of this research. B.S. thanks the Brussels Region for support through the program “Brains Back to Brussels”.

Références

J. Emile, A. Salonen, B. Dollet, and A. Saint-Jalmes, Langmuir **25**, 13412 (2009).

B. Scheid, J. Delacotte, B. Dollet, E. Rio, F. Restagno, E. van Nierop, I. Cantat, D. Langevin, and H. Stone, Europhys. Lett. **90**, 24002 (2010).

S. Dorbolo, E. Reyssat, N. Vandewalle, and D. Quéré, Europhys. Lett. **69**, 966 (2005).

S. Dorbolo, D. Terwagne, R. Delhalle, J. Dujardin, N. Huet, N. Vandewalle, and N. Denkov, Coll. and Surf. A **365**, 43 (2010).

K. J. Stebe, S.-Y. Lin, and C. Maldarelli, Phys. Fluids A **3**, 3 (1991).

S. Naire, R. J. Braun, and S. A. Snow, Phys. Fluids **13**, 2492 (2001).

K. Golemanov, N. Denkov, S. Tcholakova, M. Vethamuthu, and A. Lips, Langmuir **24**, 9956 (2008).

E. Lauga, M. Brenner, and H. Stone, in *Handbook of Experimental FLuid Dynamics*, edited by C. Tropea, A. Yarin, and J. Foss (2007), pp. 1219–1240.

A. Maali and B. Bhushan, Phys. Rev. E **78**, 027302 (2008).

C. Kunert and J. Harting, Prog. Comp. Fluid Dyn. **8**, 197 (2008).

C. Stenvot and D. Langevin, Langmuir **4**, 1179 (1988).

J. Petkov, K. Danov, and N. Denkov, Langmuir **12**, 2650 (1996).